Brain Struct Funct (2012) 217:127–139
DOI 10.1007/s00429-011-0325-x

ORIGINAL ARTICLE

Quantitative in vivo MRI measurement of cortical development in the fetus

Cédric Clouchoux · Dimitri Kudelski · Ali Gholipour · Simon K. Warfield · Sophie Viseur · Marine Bouyssi-Kobar · Jean-Luc Mari · Alan C. Evans · Adre J. du Plessis · Catherine Limperopoulos

Received: 24 January 2011 / Accepted: 28 April 2011 / Published online: 12 May 2011

Abstract Normal brain development is associated with expansion and folding of the cerebral cortex following a highly orchestrated sequence of gyral–sulcal formation. Although several studies have described the evolution of cerebral cortical development ex vivo or ex utero, to date, very few studies have characterized and quantified the gyrification process for the in vivo fetal brain. Recent advances in fetal magnetic resonance imaging and post-processing computational methods are providing new insights into fetal brain maturation in vivo. In this study, we investigate the in vivo fetal cortical folding pattern in healthy fetuses between 25 and 35 weeks gestational age using 3-D reconstructed fetal cortical surfaces. We describe the in vivo fetal gyrification process using a robust feature extraction algorithm applied directly on the cortical surface, providing an explicit delineation of the sulcal pattern during fetal brain development. We also delineate cortical surface measures, including surface area and gyrification index. Our data support an exuberant third trimester gyrification process and suggest a non-linear evolution of sulcal development. The availability of normative indices of cerebral cortical developing in the living fetus may provide critical insights on the timing and progression of impaired cerebral development in the high-risk fetus.

Keywords Brain development · Cortical surface · Fetal · Gyrification · MRI

C. Clouchoux · M. Bouyssi-Kobar · C. Limperopoulos (✉)
Division of Diagnostic Imaging and Radiology,
Children's National Medical Center, Washington, DC, USA
e-mail: climpero@cnmc.org

C. Clouchoux · A. C. Evans · C. Limperopoulos
McConnell Brain Imaging Center, Montreal Neurological Institute, McGill University, Montreal, QC, Canada

D. Kudelski · J.-L. Mari
LSIS, UMC CNRS 6168, Université de la Méditerranée, Marseilles, France

D. Kudelski · S. Viseur
GSRC, EA 4234, Université de Provence, Marseilles, France

A. Gholipour · S. K. Warfield
Department of Radiology, Harvard Medical School, Children's Hospital Boston, Boston, MA, USA

A. J. du Plessis · C. Limperopoulos
Division of Fetal and Transitional Medicine, Children's National Medical Center, Washington, DC, USA

C. Limperopoulos
Department of Neurology and Neurosurgery, McGill University, Montreal, QC, Canada

Introduction

Recent advances in fetal magnetic resonance imaging (MRI) (Jiang et al. 2007) and post-processing computational methods (Rousseau et al. 2006; Jiang et al. 2007; Guizard et al. 2008; Gholipour et al. 2010a; Clouchoux et al. 2010b) are providing important new insights into fetal brain maturation in vivo. However, quantification of in vivo fetal brain development remains a major challenge, mainly due to fetal motion during the acquisition phase and the inherent low tissue contrast of the immature brain (Prayer 2006; Garel 2008).

A number of recent studies have characterized total and regional brain volume in the living fetus (Limperopoulos et al. 2010; Gholipour et al. 2010b; Grossman et al. 2006; Kazan-Tannus et al. 2007). However, very few studies have delineated in vivo fetal cerebral cortical development. The first ex vivo study was reported by Chi et al. (1977),

who described the timing of fetal sulcation using manual outlining. Similar observations have been made by Garel et al. (2001), where MRI was used to investigate the timetable of cortical development in a cohort of 173 normal fetuses from 22 to 38 weeks gestational age (GA). More recently, studies have focused on delineating the developing cortical surface using a three-dimensional reconstruction, in order to extract precise and reproducible measurements (e.g., cortical curvature). Batchelor et al. (2002) described the folding process in ten ex vivo fetuses between 19 and 40 weeks of gestation. Dubois and colleagues (2008a) provided one of the first descriptions of in vivo cerebral gyrification from 26 to 35 weeks GA; however, this work was conducted on ex utero premature infants. Awate et al. (2009) described cortical development in newborns between 1 and 2 weeks of age, using a combination of shape indexes computed on the cortical surface. In the only previous study of cortical folding in the living fetus, Hu et al. (2009) described cortical development over a broad range of gestation (21–37 weeks), but did not extract fetal cortical surfaces, precluding therefore explicit delineation of the cortical folding pattern. Similarly, Kasprian et al. (2011) characterized the cortical shape in the in vivo fetus in order to assess the origins of hemispheric asymmetries. Noteworthy is the fact that this was carried out without reconstruction of the fetal cortical surface. The most recent quantification of in vivo fetal brain development was described by Corbett-Detig and colleagues (2011) in 21 fetuses between 20.57 and 25.86 weeks GA. Although this investigation provides important insights on the global and regional development of the subplate, including changes in cortical plate thickness, it focuses on a narrow second trimester gestational age range, at a time when important developmental events (such as the delineation of primary and secondary folds) have yet to occur.

The primary objective of the current study was to investigate cerebral cortical folding in the healthy in utero brain between 25 and 35 weeks GA using advanced cortical surface feature extraction. This timeframe is a critical period in human brain development, due to the explosive gyrification occurring at the end of the second trimester and during the third trimester. Specifically, we sought to describe the evolution of the cerebral cortical gyrification using reconstructed cortical surfaces extracted from manually corrected segmentations of the developing fetal white matter. From these surfaces, a set of cortical measures were derived, including the gyrification index (GI) (Luders et al. 2006) and cortical surface area. In addition, we developed a specific features extraction algorithm, which identifies the sulcal fundi thereby allowing the measurement of evolving sulcal organization (Clouchoux et al. 2010c).

Materials and methods

Subjects and MRI procedure

We studied 12 healthy fetuses from 25.2 to 35.1 weeks GA. All pregnant women were healthy volunteers. We excluded pregnant women with multiple gestations, congenital infection, or any maternal contraindication to MRI. We also excluded any fetus with brain dysgenesis or other systemic anomalies by antenatal ultrasound, as well as those with chromosomal abnormalities by amniocentesis. All fetuses were studied by MRI scans performed on a 1.5-T scanner (Achiva, Philips Medical System, Netherlands) and a 5-channel phased-array cardiac coil. Multiplanar single-shot turbo spin echo imaging was performed (echo $\text{time}_{\text{eff}} = 120$ ms, repetition time $= 12{,}500$ ms, 0.625 signal averages, 330-mm field of view, 2-mm slice thickness, no interslice gap, 256×204 acquisition matrix, acquisition time 30–60 s). After birth, all subjects also had normal postnatal MRI studies. Multiplanar acquisitions (axial, coronal and sagittal) provided multiple in-plane high-resolution volumes along the three principal axes (mean number of acquisitions for each subject was 8.0 ± 2.0; range 6–10). No maternal sedation was used. Gestational ages were estimated using maternal dates or, when available, using first-trimester ultrasound measurements (Limperopoulos et al. 2010). The study was approved by the Boston Children's Hospital Committee on Clinical Investigation and written informed consent was obtained from all the participants.

Image processing stage

Quantification of in vivo fetal brain development is technically challenging (Limperopoulos and Clouchoux 2009; Rousseau et al. 2006; Jiang et al. 2007; Habas et al. 2010). Ultrafast T2-weighted MR images provide good contrast between the different developing cerebral tissues, however, combined fetal and maternal motion during data acquisition results in image degradation (Jiang et al. 2007; Rousseau et al. 2006; Clouchoux et al. 2010b; Gholipour et al. 2010a). Consequently, advanced computational methods are required to create high-resolution fetal MR images. Although a large number of image processing tools exist for the adult, these are generally not suitable for fetal MR imaging, due to the image degradation, poor signal-to-noise ration (SNR), resolution, tissue contrast and dense signal difference at the brain and scalp interface (Jiang et al. 2007; Rousseau et al. 2006). Recent advances in fetal imaging now provide a set of algorithms specifically dedicated to fetal MR image processing (Rousseau et al. 2006; Jiang et al. 2007; Clouchoux et al. 2010b; Gholipour et al. 2010a). We describe in the current paper the processing

methods used to enhance the overall image quality of all fetal MRI scans performed during this study.

T2 volume correction

Mixed fetal and maternal motion limits image resolution and tissue contrast. Different post-processing techniques have been proposed to compensate for such motion artifact (Rousseau et al. 2006; Jiang et al. 2007; Gholipour et al. 2010a; Clouchoux et al. 2010b) using multiplanar fetal acquisitions in order to correct inter-slice motion. These multiplanar images are then used to reconstruct the missing or corrupted information, providing access to a high-resolution fetal volume. In our study, each fetal brain was scanned at least once in each of the three principal planes (sagittal, coronal, axial). The tissue volumes were then corrected for non-uniformity and intensity normalized (Sled et al. 1998). Next, all fetal MRI scans were subjected to a previously validated super-resolution reconstruction algorithm (Gholipour et al. 2010a), based on a motion estimation algorithm. More precisely, this super-resolution reconstruction method uses both maximum likelihood and robust motion estimation error minimization. For each fetal brain, motion was estimated by comparing each acquired slice and a reconstructed slice-model (error function minimization). Specifically, a single 6-degrees of freedom (DOF) rigid transformation was computed for each slice toward the target volume. This slice-to-volume registration stage used a multi-level registration framework, registering a reduced stack of slices at each stage. Super-resolution volumes were then reconstructed using an iterative scheme based on a slice-to-volume registration method and scattered data interpolation. The enhanced reconstructed fetal MR images then provide the necessary tissue contrast required for accurate segmentation of the cerebral folds (Fig. 1a).

White matter segmentation

Segmentation of the developing white matter with accurate delineation of the inner surface of the cortical plate is essential for successful measurement of folding in the developing third trimester fetal brain. To study cortical gyrification, the inner surface of the cortical plate is preferred, given that the outer surface is unstable (Rivière et al. 2002). The outer surface of the cortical plate is also less convoluted than the inner surface, which can lead to sulcal narrowness. Therefore, in this study, the white matter encompassed several lamination layers, including unmyelinated white matter, subplate, intermediate layer and myelinated white matter, depending on the gestational age (Kostovic and Judas 2002). In vivo fetal brain tissue segmentation is a very complex problem (Habas et al. 2010), even with high-resolution image reconstruction, primarily because of the inherently low contrast between fetal brain tissue types. An atlas-based segmentation method based on manual delineation of fetal brain tissues has been described (Habas et al. 2010), that facilitates in vivo fetal brain tissue segmentation. However, to date, fetal brain segmentation has been described over a very narrow gestational age window, i.e., from 20.5 to 24.7 weeks (Habas et al. 2010), over which the fetal cortical surface remains relatively smooth and simplified. With the growing complexity of the cortical surface particularly from 27 weeks onward, tissue segmentation algorithms are increasingly challenged (Rousseau et al. 2006).

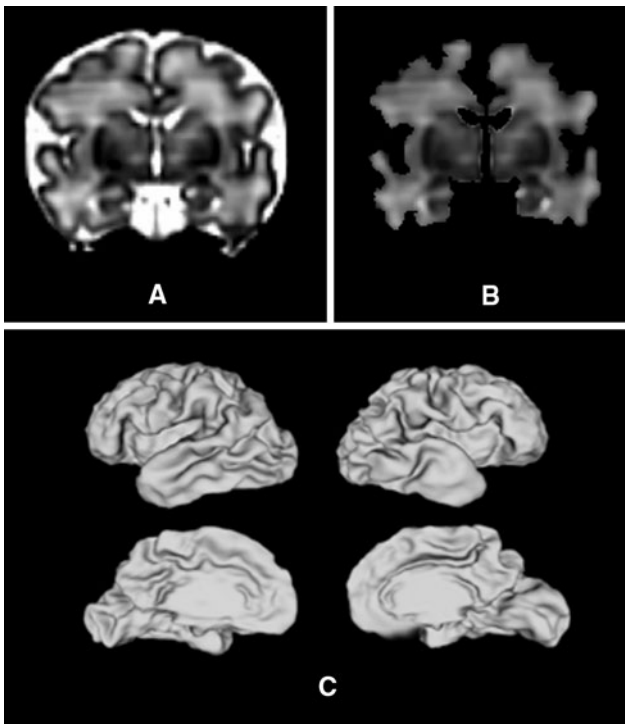

Fig. 1 Example of a fetal brain (33 weeks GA). **a** High-resolution reconstructed brain (1 × 1 × 1 mm). **b** Brain mask used to reconstruct the inner cortical surface. **c** Reconstructed inner cortical surface for left and right hemispheres

To facilitate the manual delineation of the inner surface of the cortical plate, we implemented an algorithm aimed at extracting an initial approximation of the white matter, using an atlas-based tissue segmentation method (Guizard et al. 2008). Manual segmentation of the developing white matter was first defined on a corresponding age-dependent fetal atlas using a two-step procedure (Guizard et al. 2008). For each subject, the corresponding atlas was linearly registered to the acquired volume (9 DOF, rotation, translation, and scaling in the three directions). Having achieved a reasonable match with this linear step, the atlas could then be reliably non-linearly registered to the subject to achieve an improved match. For each subject, the

transformation matrices of these two registration steps were then used to register the segmented white matter to the fetal brain.

As a comparison, we applied the segmentation method described by Zhang et al. (2001), using a hidden Markov random field and expectation maximization algorithm (in our case, the manually segmented age-dependent fetal atlas was used as the a priori atlas). Applying this segmentation method (Zhang et al. 2001) did not visually improve the segmentation result, in comparison to our atlas-based approach. In three cases, the accuracy of the white matter delineation was visibly better. We also calculated the Dice index (Dice 1945) to measure the overlap between the manually corrected segmentations and the automatically generated segmentation results, and compared the dice coefficients. The results showed that for 9 out of the 12 subjects, the Dice score was very similar between the two segmentations algorithms (0.79–0.84 for the method proposed by Zhang; 0.80–0.84 for our segmentation method). However, for three of the subjects, the overlap measure was higher using our segmentation method, than the one used by Zhang (>0.80 for our method vs. <0.74 for Zhang's method). Therefore, we chose to use the segmentation process described in our paper.

To obtain an accurate representation of the cortical plate, the resulting segmentations were manually corrected by two independent operators. The manual corrections were repeated twice by two trained operators (C.C and M.B.K), and the volume of each segmentation was used to determine inter- and intra-observer correlation coefficients (Cohen 1960) for the white matter extraction. The inter-rater correlation was >0.95, and intra-rater correlations for manual segmentations ranged from 0.97 to 0.98 for the white matter volumes. The overlap between manual corrections was also evaluated using the Dice coefficient. Inter-rater overlap Dice scores ranged from 0.94 to 0.98, and intra-rater scores ranged from 0.95 to 0.98.

Figure 1b illustrates the segmented developing white matter after the pre-processing stages. A morphological closing was then applied to this volume. By including the subcortical gray matter and the ventricles to the developing white matter mask, this morphological operation enabled us to define the inter-hemispheric cut and, therefore, to obtain a topologically correct mesh (spherical) (Fischl et al. 1999).

Inner surface of cortical plate extraction

The inner surface of the cortical plate was extracted using CLASP (McDonald et al. 2000), based on a spherical-mesh deformation algorithm. In a previous study (Lee et al. 2006), it has been shown that CLASP was more accurate than other cortical surface extraction methods in representing both the cortical anatomy and optimizing the mesh topology. A mesh composed of 10,240 vertices (20,480 triangles) was generated from the segmentation, for each hemisphere. Figure 1c represents a typical inner cortical surface obtained from a 33 week GA fetus. All the meshes were then registered together and resampled (McDonald et al. 2000), in order to reduce the inter-subject anatomical variability due to an incorrect vertices sampling. This registration operation performs a hierarchical deformable registration of the meshes using a multi-scale approach. It combines a regularization step, preserving the local mesh topology, and an iterative local search for the optimal vertex correspondence based on feature field matching (Boucher et al. 2009). For each hemisphere, we then computed two components of fetal cortical growth, i.e., cortical depth (Boucher et al. 2009) and the gyrification index (Zilles et al. 1988; Luders et al. 2006).

Sulcal features extraction

Differential quantities reliably describe the local geometry of a surface. Among them, the second-order values, such as principal curvatures, k_1 and k_2, and principal directions, $\overrightarrow{t}_1$ and $\overrightarrow{t}_2$, play a crucial role in ridge detection. Traditional approaches for ridge detection then rely on third-order differential quantities (i.e., curvature derivatives). However, these techniques are limited by a common problem, i.e., both are dependent on 'noise', surface meshing, and local aspects of the geometry, which may lead to inconsistencies in feature extraction algorithms. Moreover, results obtained using such methods result in non-connectivity in their shape (Yoshizawa et al. 2005). The connectivity ensures that all the points, or vertices, of a graph are linked together. In Kudelski et al. (2010), the connectivity is assured using a vertex labeling step and mathematical morphological operators to extract feature lines. As these operators respect the topology of the objects, the connectivity of the resulting feature lines is guaranteed. Kudelski and colleagues (2010) propose the use of parameterization to represent a feature region into a 2D regular grid. Therefore, the line extraction process is achieved using classical operators stemming from the image processing domain and mapping back the 2D skeleton on the 3D region by inverse parameterization. The main drawback of this method is the convergence and the distortion of the parameterization. For these reason, we performed the skeleton extraction directly from the 3D feature region.

In order to ensure such connectivity, we applied ridge detection to extract the sulcal pattern. First, we applied a noise-reduction algorithm on the curvature maps. Then, each vertex was labeled in order to define regions of interest (Kudelski et al. 2010). Finally, the sulcal lines were extracted from these regions using topological operators to ensure the connectivity of the extracted lines.

The initial step of ridge detection method estimates the principal curvature of the surface. To deal with noise, we first applied a Laplacian smoothing of the point coordinates. The point coordinates are then restored to perform the sulci detection on the original geometry with smoothed curvature values. The estimation of k_1 and k_2 is done by the method proposed in Goldfeather and Interrante (2004) due to its quality and robust results (Gatzke and Grimm 2006). The methods aim to fit locally a bi-cubic polynomial in the least-squares sense:

$$f(x,y) = \frac{A}{2}x^2 + Bxy + \frac{C}{2}y^2 + Dx^3 + Ex^2y + Fxy^2 + Gy^3$$

to build the matrix of the second fundamental form W:

$$W = \begin{bmatrix} A & B \\ B & C \end{bmatrix}$$

k_1 and k_2 correspond to the largest eigenvalues of W (with $|k_1| > |k_2|$). From k_1 and k_2, two shape descriptors are then defined: the mean curvature H and the Gaussian curvature K where:

$$H = \frac{k_1 + k_2}{2} \text{ and } K = k_1 \cdot k_2$$

From the signs of H and K, points are classified into eight types of basic shapes (see Fig. 2).

Sulci are located in the concave parts of the surface, where $H > 0$, as depicted in the bottom row of Fig. 2. It is then possible to use the curvature estimation to label each point p_i as:

$$\text{label}(p_i) = \begin{cases} 1 & \text{if } H > 0, \\ 0 & \text{otherwise} \end{cases}$$

For the sake of clarity, we denoted F as the set of points labeled as 1, p a point of the surface and q_i its direct neighbors. The local geometry is then transformed into a binary map corresponding to regions of interest (with $H > 0$ for all included vertices), and the labeled points characterize the sulcal pattern (Fig. 3). As a result, the algorithm turns the regions of interest into skeletal curves, representing sulcal fundi.

Once all the points have been labeled, the goal is then to obtain the skeleton of each region directly on the mesh. Characterizing a 2D shape is challenging for a number of reasons. Classical approaches resolve this characterization problem using a skeleton (Jain 1989) to describe the geometry, the topology, and the connectivity of a set, and then applying this skeleton to extract sulci from the 3D regions. The extraction of the sulcal pattern from a skeleton-based technique turns out to be an elegant and robust solution, as it guarantees connectivity and characterizes the geometry and the topology of the features described. Moreover, the final points describing the concave parts are enclosed into a subset leading to a concise representation of the sulcal pattern. For these reasons, we chose this skeleton-based approach to describe the sulcal pattern in our fetal studies.

To reduce the regions of interest to skeletons, we selected the morphological operators proposed by Rössl et al. (2000). The skeleton was then computed by an iterative thinning process (i.e., successive erosion without modification of the topology). We then modified the original algorithm as follows:

First, we classified each point into four categories (instead of three in the original algorithm: disk, center, complex and outlier; Fig. 3a). p is considered the center if p and all its neighbors q_i belong to F. In this case, all q_i are marked as disks. This corresponds to the definition of a simple point (i.e., a point that does not change the topology if it is removed). Conversely, p is a complex point when

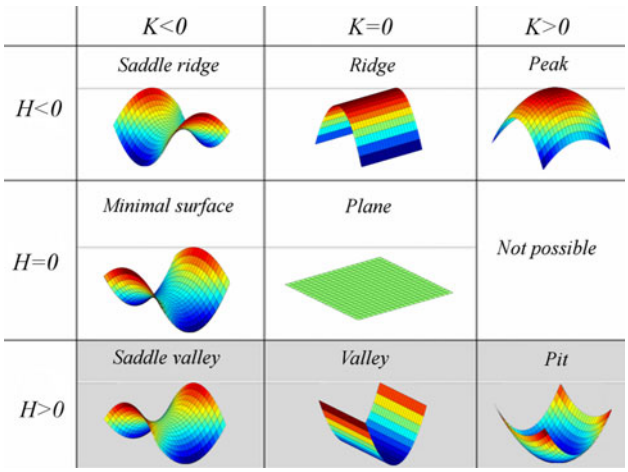

Fig. 2 Basic shapes defined by the signs of mean and Gaussian curvatures

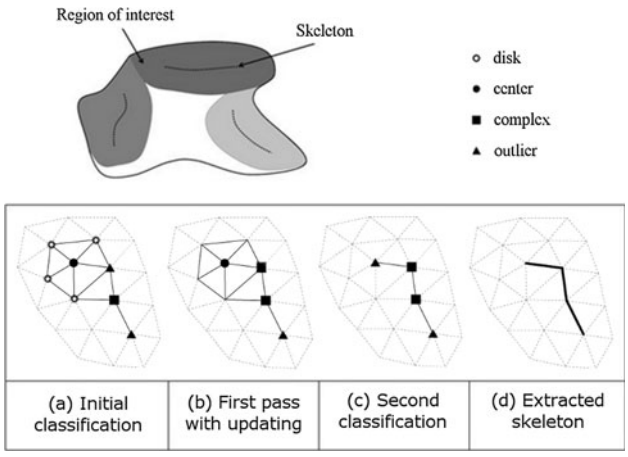

Fig. 3 Illustration of the skeletonization process. *Top* Scheme of the skeletonization of region of interest. *Bottom* Detail of the skeletonization steps on the mesh

there exists at least four transitions among its neighbors q_i. Removing a complex point would result in a change in the topology, as it would break a single line into two lines. A transition is defined as:

$$\text{label}(q_i) \neq \text{label}(q_{i+1})$$

where label represents the category of the point topology. Then, all the remaining points are flagged as outlier points.

We modified the thinning method of the original algorithm to match our definition of the extracted feature and to ensure connectivity during the computation of the skeleton. This process was accomplished in three steps. First, all points marked as disks were removed since they do not modify the topology. Then, during the sequence, for each point deleted, the classification of its neighbors q_i was updated. In this way, the topology was not modified and the connectivity of the obtained feature was ensured. This step was not implemented in the original algorithm but was added as a new feature, in order to avoid ruptures in the topology (i.e., skeletons fragmented in several parts). The process was iterated until it converged. The final step consisted of removing all outlier points with at least two neighbors belonging to F because they do not alter the topology. Figure 3 illustrates each different step of the thinning process from the classification (Fig. 3a) to the convergence (Fig. 3d). Figure 4 shows the resulting sulcal lines on two fetal brains.

Age-dependent cortical fetal templates

The fetal brain shape and size are too variable over time to compute a single template. Given that the brain is rapidly evolving in size and shape in utero, particularly during the third trimester, creating an average cortical surface would be technically challenging and theoretically questionable, because of the difficulty in matching unfolded (early) and folded (later) cortical surfaces. However, templates are very useful, as they provide a representation of the average anatomy in a given population (Evans et al. 2006; Fischl et al. 1999). Therefore, in order to provide a more generic representation of different stages in the gyrification process, we created four cortical surface templates. We first divided our fetal subjects into four GA groups: 25–28 weeks GA, 28–30 weeks GA, 30–32 weeks GA and 32–35 weeks GA. For each group, we then generated an unbiased cortical plate template, using the method described in Lyttelton et al. (2007). Briefly, the template construction relies on an iterative registration of the cortical surfaces. For each iteration, an average surface is computed for all the subjects. Then, each subject is registered to this average, and a new average surface is computed, and used as a target for the next iteration. This registration algorithm has been previously described (McDonald et al. 2000). This process allows us to overcome the inter-individual variability, exhibiting the average shape characteristics of the cortical plate in the defined groups (Lyttelton et al. 2007). Therefore, the gross anatomical characteristics of the brain are clearly visible (Lyttelton et al. 2007). Of note, each defined gestational age range included three subjects (six hemispheres), corresponding to a particular set of neurodevelopmental events, as described in (O'Rahilly and Muller 1999).

Probability maps of the sulci localization were generated using the features extraction maps described above. Each feature map was then smoothed using a full width half maximum (FWHM) of 2 mm. We compared these maps with cortical depth average maps (Boucher et al. 2009). Although cortical depth provides useful information when characterizing the overall folding pattern, the features extraction method described here provides detailed information about the folding process that cannot be elucidated using the depth map.

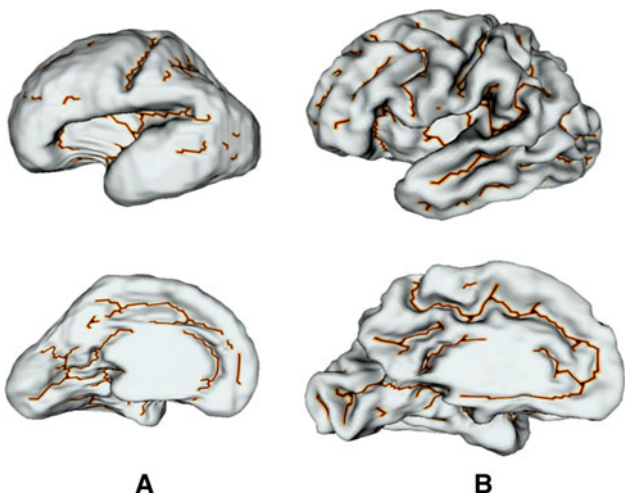

Fig. 4 Examples of feature extraction in two fetuses at 27.3 weeks GA (**a**) and at 33.1 weeks GA (**b**). The complexity of the sulcal pattern increases with gestational age. *Lines* indicate the sulcal skeleton

Quantification of gyrification

To obtain a complete representation of the gyrification process, we computed the GI of all the cerebral hemispheres in our cohort. The GI was first defined as a two-dimensional measure (Zilles et al. 1988), but was further refined in order to be applicable to the recent three-dimensional reconstruction of the cortical surfaces (Luders et al. 2006). It measures the ratio between the cortical surface area and the cortical surface convex hull, and provides a quantification of the folding state of the considered surface.

We also computed the cortical plate area for each hemisphere. This area is defined by the sum of the area of each triangle composing the cortical mesh.

Results

Qualitative description of the gyrification process in the fetus

The three-dimensional cortical surface representation enabled us to delineate sulcal organization between 25 and 35 weeks GA. Figure 5 illustrates the important morphological changes occurring between 25.2 and 35.1 weeks of gestation. The folding pattern evolution is characterized by increasing complexity from 25 to 35 weeks GA. Specifically, at 25 weeks, the cortical plate is very smooth, and no major sulcus is clearly delineated, except in the insular region where the operculation process has already started. From 28 weeks GA, the cortical plate begins to be more convoluted, with an increased complexity occurring from 30 weeks GA, where secondary sulci begin to be delineated. The timetable of the sulcation is described hereafter. The first folding occurs at the insula, which is noted as early as 25 weeks GA, although the operculation process is delayed until around 28 weeks GA. The central sulcus (CS) is already formed, although it is very narrow at 25 weeks GA. Between 25 and 27 weeks, the superior temporal sulcus (STS), calcarine fissure (Calc.), parieto-occipital fissure (POF), and the calloso-marginal fissure (CMF) are first seen, and are well formed by 28–29 weeks GA. The collateral sulcus is formed at 28 weeks. The frontal sulci are clearly visible from

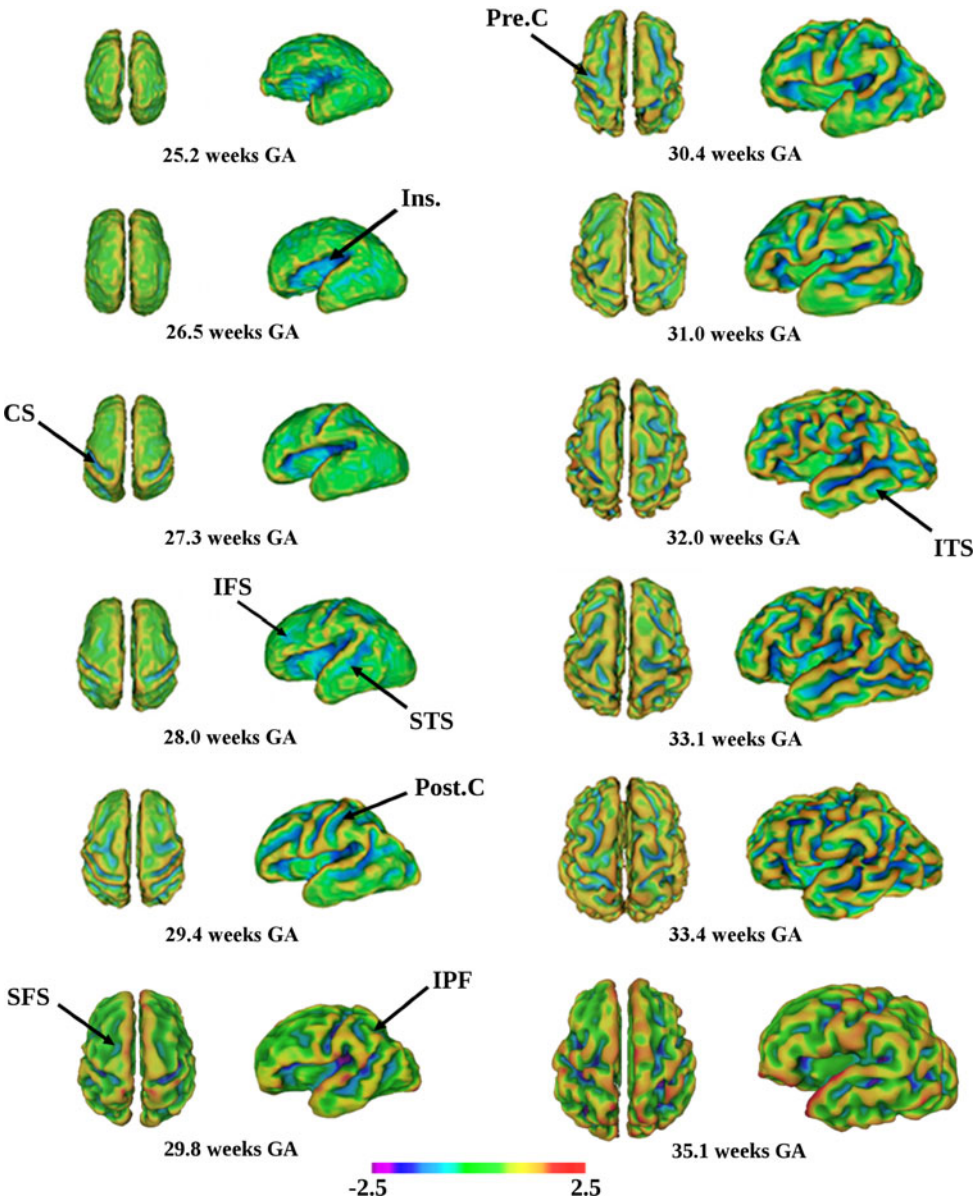

Fig. 5 Inner cortical surfaces of fetuses from 25.2 to 35.1 weeks GA. *Colors* represent sulcal depth (Boucher et al. 2009). Visible sulci are displayed including: Insula (*Ins.*), central sulcus (*CS*), inferior frontal sulcus (*IFS*), superior temporal sulcus (*STS*), post-central sulcus (*Post. C*), superior frontal sulcus (*SFS*), intra-parietal fissure (*IPF*), pre-central sulcus (*Pre. C*), and inferior temporal sulcus (*ITS*)

27 weeks. In the parietal lobe, the intra-parietal fissure (IPF) appears very early, from 27 weeks GA. After this folding, the post-central sulcus appears, making more complex the sulcal pattern in the parietal lobe. The inferior and superior sulci folding in the frontal lobe appears around the 28th week of gestation, while the pre-central sulcus is present from the 29th week. The inferior temporal sulcus is visible from the 29th week, although it is clearly delineated at 30st weeks. Secondary sulci also appear before birth, including the orbital and olfactory sulci becoming visible at the 30th week GA. After 31 weeks, the folding pattern of previously formed sulci becomes more complex, such as the folds in the cingulate gyrus, especially the frontal part of the calloso-marginal fissure.

Age-dependent cortical fetal template

The four age-dependent cortical templates show the gross anatomical changes occurring in the gyrification of the fetal cortical plate (Figs. 6, 7). The timetable of the sulcation is very well illustrated by the combination of these four atlases and the corresponding sulci probability maps, as shown in Fig. 6. Figure 6 also illustrates the evolution of the sulcal complexity, displayed on a spherical representation of the cortical surface, in order to better appreciate the evolution of the folding pattern in a same referential.

The probability maps of the sulcation provide a quantitative evaluation of the evolving cortical folding state during the gyrification process. These maps and their associated templates clearly illustrate the early appearance of the primary sulci (CS, STS, CMF) from 25/27 weeks GA, as well as the subsequent formation of the secondary folds (orbital, olfactory, cingular sulci) from the 30st week of gestation. Figure 7 demonstrates the average sulcal depth between 25 and 35 weeks GA on the corresponding age-dependant fetal templates using the depth potential function (Boucher et al. 2009).

Quantification of the gyrification index in the fetus

In our study, the observed gyrification index evolution is not linear, and confirms that the folding process is

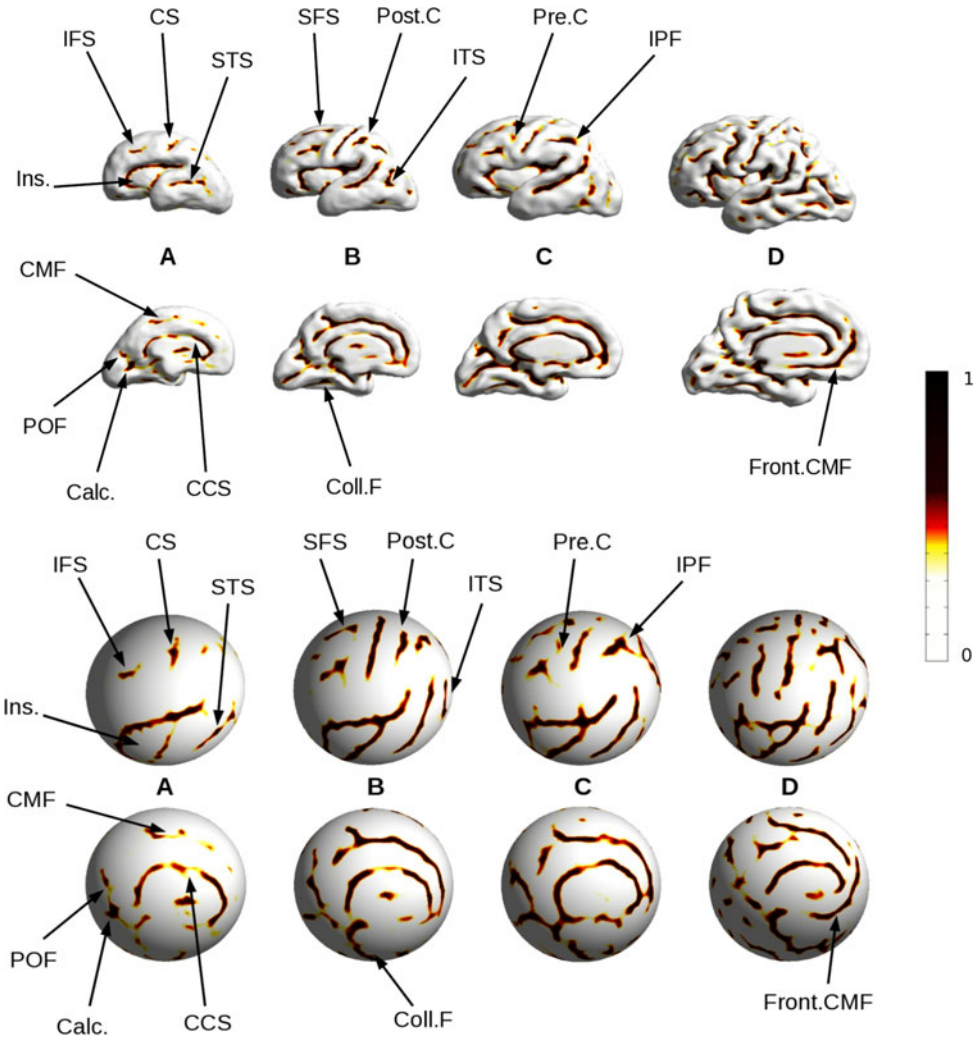

Fig. 6 Probability map of sulci location during growth using the proposed features extraction method. The fetal brains were divided into four gestational age groups: 25–28 weeks GA (**a**), 28–30 weeks GA (**b**), 30–32 weeks GA (**c**), 32–35 weeks GA (**d**). *Top* group-averages of the cortical plate reconstructed surfaces. *Bottom* spherical representation of the cortical surface averages, in order to compare the folding process on a same referential. The main sulci are displayed, including: inferior frontal sulcus (*IFS*), central sulcus (*CS*), superior temporal sulcus (*STS*), insula (*Ins.*), calloso-marginal fissure (*CMF*), calcarine fissure (*Calc.*), parieto-occipital fissure (*POF*), corpus callosum sulcus (*CCS*), superior frontal sulcus (*SFS*), post-central sulcus (*Post. C*), inferior temporal sulcus (*ITS*), collateral fissure (*Coll. F*), pre-central sulcus (*Pre. C*), intra-parietal fissure (*IPF*), frontal calloso-marginal fissure (*Front. CMF*)

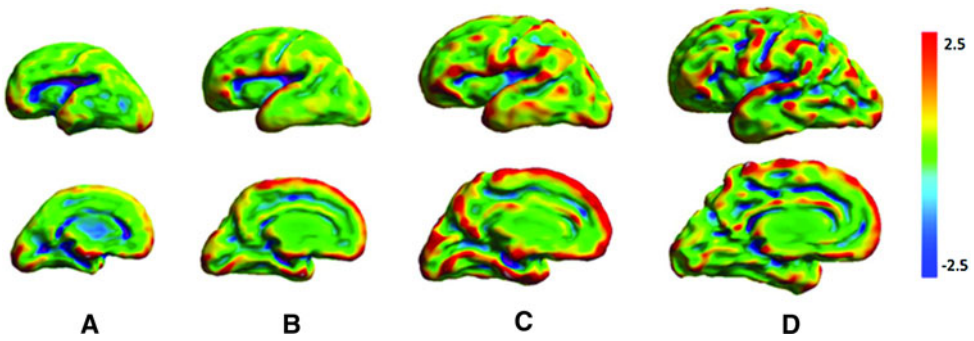

Fig. 7 Average sulcal depth between 25 and 35 weeks GA represented on the age-dependant fetal templates using the depth potential function proposed by Boucher et al. 2009

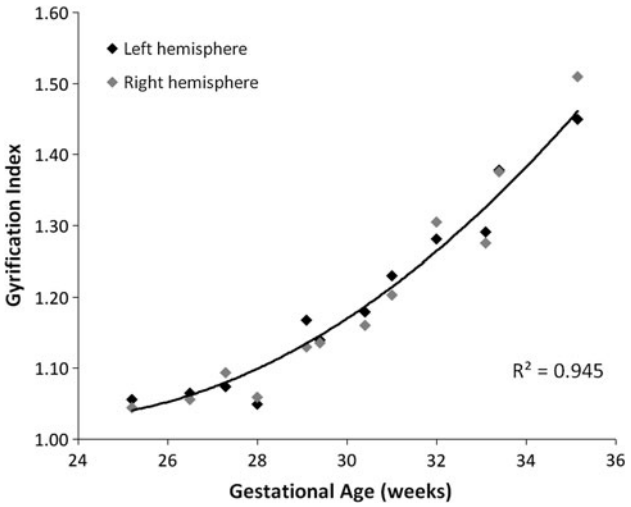

Fig. 8 Gyrification index computed on each cerebral hemisphere for all 12 fetuses, with second-order polynomial interpolation

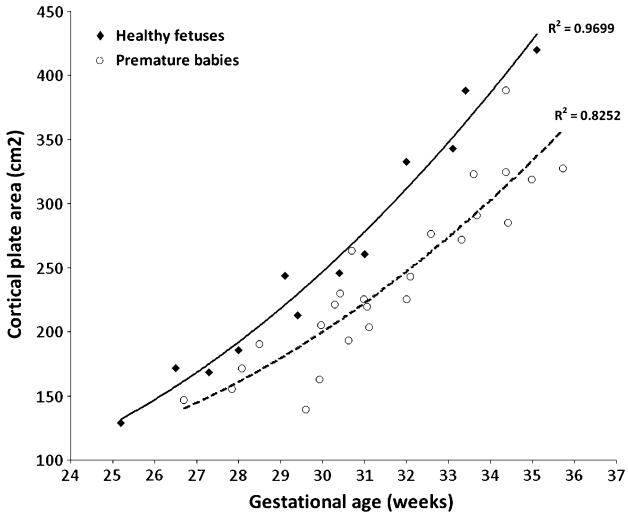

Fig. 9 Inner cortical plate area of fetuses (*solid line*), and *ex utero* premature infants (*dashed line*) (Dubois et al. 2008a), with second-order polynomial interpolation

accelerated from the 28th week of gestation onward, along with the appearance of the secondary folds. Figure 8 shows the evolution of the gyrification index between 25 and 35 weeks GA, and illustrates the increased complexity of the cortical plate, occurring from the 28th week GA. This observation is supported by an increase in the inner cortical surface area across the same gestational age (Fig. 9).

Discussion

In this study, we describe our application of cortical surface reconstruction to characterize cortical folding over the critical period of peak cortical development between 25 and 35 weeks gestation. First, we apply processing algorithms to the in vivo fetal MR images to improve contrast, to reduce motion artifact in order to enable accurate tissue segmentation. Then, in order to delineate fetal brain gyrification, we use a novel surface feature detection algorithm applied directly to the three-dimensional reconstructed fetal cortical surfaces. This algorithm provides us with an illustration of the sulcal pattern evolution during gestation. Finally, we characterize fetal cortical growth both qualitatively (i.e., visual description of the folding process) and quantitatively.

MR images enhancement and tissue segmentation

As described earlier, unsedated in vivo fetal MR images are frequently motion corrupted. As a result, the poor tissue contrast presents an obstacle when applying tissue segmentation algorithms, even when using a super-resolution method. The atlas-based segmentation method described by Habas et al. (2010) extended from 20 to 24 weeks GA and, therefore, does not address the complex changes in the fetal brain over third trimester. In the present study, we performed a first approximation of the tissue segmentation, and manual tissue delineation was required to obtain an accurate segmentation for fetal surface extraction. Although manual segmentation is a tedious and very time-consuming task (which ranged from 3 to 6 h per subject, depending on the gestational age of the fetus), it was needed to reliably extract the fetal cortical surface for older fetuses, especially those older than 30 weeks.

Sulcal features extraction

In the present work, fetal cortical surfaces were used to characterize the gyrification process. In adults, various methods have been developed to extract sulcal information (Rivière et al. 2002; Thompson et al. 1996; Fischl et al. 1999). When the external surface of the cortex is used to quantify sulcation, the extracted data are unstable across individuals given that the description is carried out using the external shapes of the sulci (Zilles et al. 1988; Regis et al. 2005). Moreover, the shallowness of the external cortical plate makes the extraction of secondary and tertiary sulci difficult; therefore, the inner surface of the cortical plate is more suitable for this purpose.

At the fetal stage of cortical development, extracting each sulcus is very complicated, mainly because no established model exists. Moreover, the current lack of a large fetal MRI dataset precludes creation of a robust database of fetal sulci. This void prevents application of neural networks algorithms used in adults (Rivière et al. 2002). Therefore, we proposed a method to extract the sulcal fundi of the inner fetal cortical surface, i.e., at the interface between cortical gray and subcortical white matter. This approach allowed us to measure the global pattern of the gyrification, and to quantify the cortical folding during the end of second and third trimesters.

The proposed sulcal features extraction method has been previously used to characterize the folding states of healthy infants between 12 and 16.8 weeks old postnatal age (Clouchoux et al. 2010c). This sulcal extraction method can also be used in a variety of clinical studies, as its primary purpose is to quantify the cortical folding, independent of age or condition (i.e., healthy vs. brain injured populations). For example, Dubois and colleagues (2008b) described a delay gyrification process in ex utero infants with intra-uterine growth restriction. The sulcal features extraction method presented herein could potentially offer new insights into the mechanisms underlying altered cortical development in intrauterine growth restricted fetuses in vivo, by quantifying precisely the onset and extent of delayed cortical plate folding. Another potential application of this method would include a quantitative comparison of cortical development in healthy in vivo fetus versus premature infants of the same gestational age. Ongoing work by our group and others is currently underway to explore these clinical relevant applications.

Age-dependent cortical fetal template

The purpose of the present work is to establish a robust methodology to quantify the developing brain's folding process, and to illustrate the gross anatomical changes that occur between 25 and 35 weeks of gestation. In this framework, we defined four age-dependent cortical fetal templates, including three subjects (six hemispheres) for each group. Such templates are very useful in illustrating gross anatomical differences between different groups of subjects. However, a larger sample size would provide a more detailed and generic description of the cortical anatomy for each template (Lyttelton et al. 2007). Such templates will also offer important reference values from which to compare fetuses at risk for impaired brain development.

Gyrification process in the fetus

Although not ideal, data from the ex vivo studies provide valuable reference points for comparison with in vivo studies of fetal brain development (Chi et al. 1977; Armstrong et al. 1995; Guihard-Costa and Larroche 1990; Shankle et al. 1998). Of the few studies addressing maturation of the fetal cortex in ex vivo fetuses (Batchelor et al. 2002; Zhang et al. 2010), one study (Batchelor et al. 2002) had no subjects between 27 and 36 weeks GA, and the other (Zhang et al. 2010) had measurements limited to the axial plane, precluding measurement of overall brain volume. Despite these limitations, both the studies describe a gyrification process that is similar to ours.

Our findings corroborate previously described in vivo fetal cortical development studies (Garel et al. 2001; Hu et al. 2009). The timetable of the gyrification described by Garel et al. (2001) is also in accordance with our findings for the majority of the folds. However, with one notable difference, occurring in the calloso-marginal area, which is not visible before 27 weeks GA in our study, although this region is already folded at this GA according to Garel et al. (2001). One possible reason for this difference may relate to the narrowness of this fold at the first stage of gyrification in which our sulcal detection method may have failed to detect it. Another possibility may relate to our small sample size. When comparing our results to Hu and colleagues (2009), the different measures performed on the in vivo fetal cortical surfaces show a comparable pattern of the evolving complexity of the gyrification to our data.

In Chi et al. (1977), observations of the gyrification in post mortem fetuses are reported. Although our findings are comparable to most of the observations described by Chi et al. (specifically in the frontal and temporal lobes), there are some differences in the appearance of certain sulci. For example, the cingulate and the olfactive sulci are described as early as 16–17 weeks GA postmortem, however, we detected these sulci after 30 weeks GA. The difference in appearance of these sulci may be explained by the fact that Chi and colleagues described the gestational age of sulci when these sulci where present in 25–50% of the subjects. In the present study, we rely on probability maps using

very precise sulcal fundi information, which may in turn be more restrictive. Specifically, we describe the gestational age at which a sulcus appears when this sulcus is present in over 50% of the subjects.

Our data corroborate those of Dubois et al. (2008a) who described cortical development in preterm infants over a similar gestational age range (i.e., 25–35 weeks GA). Specifically, the sequence of sulcal development in our fetal studies was similar to that in the equivalent gestational age premature infants in their study (Dubois et al. 2008a). In both the ex utero premature and in vivo fetal brain, the gyrification process as measured by the gyrification index and the cortical surface area, accelerates and becomes increasingly complex after 28–30 weeks GA.

Although caution should be exercised when comparing our findings in the fetus with ex utero premature infants (Dubois et al. 2008a), several interesting differences are apparent between ex utero and in utero cortical development. Developmental differences in cortical surface area in relation to the stage of gyrification (Fig. 9) suggest a progressive third trimester deceleration in cortical surface area growth in the premature ex utero brain compared to the in utero fetal brain. In addition, there appear to be differences in the two populations with regard to the appearance of cortical folds. Although the general order of sulcal appearance with increasing GA is similar, several notable exceptions are evident. The primary folds (insula, CS, STS, POF) as well as the pre- and post-central sulci, appear at the same stage of maturation in the two populations. However, some folds appear earlier in fetuses than in premature babies. For instance, the frontal sulci and collateral sulci are clearly formed at around 28 weeks in the fetuses, but appear at 29–30 weeks for the premature babies. This phenomenon is even more striking with the secondary sulci, such as the olfactory sulcus, which is clearly visible from 30 weeks in the healthy fetus but in some premature brains does not appear before 32 weeks. It should be noted that the method of calculating GA is not the same in the two studies. In Dubois et al. (2008a), the gestational age includes 2 weeks of amenorrhea prior to gestation. The 2 weeks of amenorrhea were not included in the gestational age calculations of our cohort. Therefore, some of the observed differences in cortical folding between healthy fetuses and premature infants might be explained by the difference in GA calculations. Nevertheless, the observed differences between the gyrification processes in the two populations suggest that further investigation is needed to examine the potential negative impact of early exposure to the extrauterine environment on cortical development in preterm infants. A larger study population is needed to confirm these intriguing findings.

Recent studies have begun to quantify asymmetries in sulci formation and in cortical morphology during ex utero and in utero brain maturation (Rajagopalan et al. 2011; Dubois et al. 2008a; Dubois et al. 2010; Hill et al. 2010; Kasprian et al. 2011). Rajagopalan and colleagues (2011), described 40 in vivo fetuses between 20 and 28 weeks GA and showed that local volumes were superior in the right hemisphere in the posterior part of the peri-Sylvian region, as well as in the frontal and post-central dorsomedial region (Rajagopalan et al. 2011). Similarly, Dubois et al. (2010) described a higher folding rate in the right hemisphere compared to the left hemisphere in ex utero preterm infants from 26 to 36 weeks of gestational age. Specifically, the superior temporal sulcus was deeper on the right side, whereas the posterior area of the sylvian region was found to be larger in the left hemisphere. Our sample size precluded us from examining asymmetries in fetal cortical development in the present study. However, ongoing work by our group is focusing on examining sulcal asymmetries using the methodology presented herein on a larger sample size.

Stability of the deep cortex and developing gyral organization

In the present study, we specifically focused our attention on the deep cortex, which has been shown to be very stable during gyrification within the same subject or across individuals (Bartley et al. 1997; Lohmann et al. 2007; Regis et al. 2005). The general idea supported by the latest developmental assumptions is that gyrification is genetically pre-determined (Rakic 1988; Regis et al. 2005). From a structural point of view, the cortical organization has been described as being stable across individuals, at the adult stage. Specifically, this stability has been described at a macroscopic level in the deep cortex (bottom of sulci), showing a reproducible organization across individuals (Regis et al. 2005; Lohmann et al. 2007; Lefebvre et al. 2009). This stable gyral organization has been subsequently modeled in adult studies (Toro and Burnod 2003; Clouchoux et al. 2010a), and is believed to be the result of a strong genetic influence (Rakic 1988; Regis et al. 2005). However, the exact mechanisms underlying cortical folding are still not clearly understood. The first hypothesis was introduced by Richman and colleagues (1975) which suggested that the formation of folds and gyri is the consequence of differences in growth rates between the different cortical layers. Although this model was at the time supported by mathematical modeling and experimental results (Barron 1950), it does not explain the consistency in the primary folding pattern (Richman et al. 1975). The second, widely accepted hypothesis has been presented by Van Essen (1997). In this important study, Van Essen proposed that cortical gyrification is driven by white matter fibers tension-based mechanisms. Interestingly, a more recent

study (Xu et al. 2010) states that the axonal tension is not directly linked to the gyrification process, supported by histological observations and tests on a finite element model of the cortical folding. Although some of these anatomical assumptions have been partly supported by adult data (Lohmann et al. 2007) and developmental models (Toro 2007), to date no study on the developing fetal brain has tested these assumptions. This is an interesting area of research that warrants further study.

In summary, we provide an in vivo description of gyral development in the human fetal brain during the critical period of rapid cortical development from 25 to 35 weeks of gestation. We propose a novel robust methodology for capturing the evolution of sulcal development during the second and third trimester that advances the quantification of cerebral cortical development in the living fetus. Our data corroborate the exuberant gyrification process occurring after 28 weeks gestation, and suggest a non-linear evolution of the sulcal pattern. Our observations support recent studies of brain maturation using ex utero MRI studies of the premature brain. However, our data also highlight the important differences between intra- and extra-uterine third trimester brain development and suggest that current extra-uterine conditions may fail to provide optimal support for third trimester cortical development. These observations warrant larger studies in these two populations.

Acknowledgments We thank Yansong Zhao and David Annese for their help with MRI applications. We are indebted to the families for participating in this study. This work was supported by the Canadian Institutes of Health Research (MOP-81116), Sickkids Foundation (XG 06-069), and Canada Research Chairs Program (Dr Limperopoulos).

References

Armstrong E, Schleicher A, Omran H, Curtis M, Zilles K (1995) The ontogeny of human gyrification. Cereb Cortex 5:56–63

Awate SP, Yushkevich P, Song Z, Licht D, Gee JC (2009) Multivariate high-dimensional cortical folding analysis, combining complexity and shape, in neonates with congenital heart disease. Inf Process Med Imaging 21:552–563

Barron DH (1950) An experimental analysis of some factors involved in the development of the fissure pattern of the cerebral cortex. J Exp Zool 113:553–581

Bartley AJ, Jones DW, Weinberger DR (1997) Genetic variability of human brain size and cortical gyral patterns. Brain 120:257–269

Batchelor PG, Castellano Smith AD, Hill DL, Hawkes DJ, Cox TC, Dean AF (2002) Measures of folding applied to the development of the human fetal brain. IEEE Trans Med Imaging 21(8): 953–965

Boucher M, Whiteside S, Evans AC (2009) Depth potential function for folding pattern representation, registration and analysis. Med Image Anal 13(2):203–214

Chi JG, Dooling EC, Gilles FH (1977) Gyral development of the human brain. Ann Neurol 1:86–93

Clouchoux C, Rivière D, Mangin JF, Operto G, Régis J, Coulon O (2010a) Model-driven parameterization of the cortical surface for localization and inter-subject matching. Neuroimage 50(2): 552–566

Clouchoux C, Coupé P, Manjon J, Guizard N, Bouyssi-Kobar M, Lefebvre M, Du Plessis AJ, Evans AC, Limperopoulos C (2010b) A novel approach for high-resolution image reconstruction for in vivo fetal brain MRI. In: Proceedings of the Sixteenth Annual Meeting of the Organization for Human Brain Mapping

Clouchoux C, Kudelski D, Bouyssi-Kobar M, Viseur S, du Plessis A, Evans AC, Mari J-L, Limperopoulos C (2010c) Cortical pattern detection for the developing brain: a 3D vertex labeling and skeletonization approach. J Med Inform Technol 16:161–166

Cohen J (1960) A coefficient for agreement for nominal scales. Educ Psychol Measur 20(1):37–46

Corbett-Detig JM, Habas PA, Scott JA, Kim K, Rajagopalan V, McQuillen PS, Barkovich AJ, Glenn OA, Studholme C (2011) 3D global and regional patterns of human fetal subplate growth determined in utero. Brain Struct Funct 215(3-4):255–263

Dice LR (1945) Measures of the amount of ecologic association between species. Ecology 26(3):297–302

Dubois J, Benders M, Cachia A, Lazeiras F, Ha-Vinh Leutcher R, Sizonenko SV, Borradori-Tolsa C, Mangin J-F, Hüppi PS (2008a) Mapping the early cortical folding process in the preterm new born brain. Cereb Cortex 18:1444–1454

Dubois J, Benders M, Borradori-Tolsa C, Cachia A, Lazeyras F, Ha-Vinh Leuchter R, Sizonenko SV, Warfield SK, Mangin JF, Hüppi PS (2008b) Primary cortical folding in the human newborn: an early marker of later functional development. Brain. 131(Pt 8):2028–2041

Dubois J, Benders M, Lazeyras F, Borradori-Tolsa C, Leuchter RH, Mangin JF, Hüppi PS (2010) Structural asymmetries of perisylvian regions in the preterm newborn. Neuroimage 52(1):32–42

Evans AC, the Brain Development Cooperative Group et al (2006) The NIH MRI study of normal brain development. NeuroImage 30(1):184–202

Fischl B, Sereno MI, Tootell R, Dale AM (1999) Cortical surface-based analysis, ii: Inflation, flattening and a surface-based coordinate system. Neuroimage 9:195–207

Garel C (2008) Fetal MRI: what is the future? Ultrasound Obstet Gynecol 31:123–128

Garel C, Chantrel E, Brisse H, Elmaleh M, Luton D, Oury J-F, Sebag G, Hassan M (2001) Fetal cerebral cortex: normal gestational landmarks identified using prenatal MR imaging. AJRN Am J Neuradiol 22(1):184–189

Gatzke T, Grimm CM (2006) Estimating curvature on triangular meshes. Int J Shape Model 12(1):1–28

Gholipour A, Estroff JA, Warfield SK (2010a) Robust super-resolution volume reconstruction from slice acquisitions: application to fetal brain MRI. IEEE Trans Med Imaging 29(10):1739–1758

Gholipour A, Estroff JA, Barnewolt CE, Connolly SA, Warfield SK (2010b) Fetal brain volumetry through MRI volumetric reconstruction and segmentation. Int J Comput Assist Radiol Surg 6(3):329–339

Goldfeather J, Interrante V (2004) A novel cubic-order algorithm for approximating principal direction vectors. ACM Trans Graph 23(1):45–63

Grossman R, Hoffman C, Mardor Y, Biegon A (2006) Quantitative MRI measurements of human fetal brain development in utero. Neuroimage 33(2):463–470

Guihard-Costa AM, Larroche JC (1990) Differential growth between the fetal brain and its infratentorial part. Early Hum Dev 23:27–40

Guizard N, Lepage C, Fonov V, Hakyemez H, Evans A, Limperopoulos C (2008) Development of fetus brain atlas from multi-axial MR acquisitions. In: Proceedings of the Sixteenth Annual

Meeting of the International Society for Magnetic Resonance in Medicine 672:132
Habas PA, Kim K, Corbett-Detig JM, Rousseau F, Glenn OA, Barkovich AJ, Studholme C (2010) A spatiotemporal atlas of MR intensity, tissue probability and shape of the fetal brain with application to segmentation. Neuroimage (in press)
Hill J, Dierker D, Neil J, Inder T, Knutsen A, Harwell J, Coalson T, Van Essen D (2010) A surface-based analysis of hemispheric asymmetries and folding of cerebral cortex in term-born human. J Neurosci 30(6):2268–2276
Hu H-H, Guo W-Y, Chen H-Y, Wang P-S, Hung C-I, Hsieh J-C, Wu Y-T (2009) Morphological regionalization using fetal magnetic resonance images of normal developing brains. Eur J Neurosci 29:1560–1567
Jain AK (1989) Fundamentals of digital image processing. Prentice-Hall, Inc, Upper Saddle River
Jiang H, Xue H, Counsell SJ, Anjari M, Allsop J, Rutherford MA, Rueckert D, Hajnal JV (2007) In utero three dimension high resolution fetal brain diffusion tensor imaging. Med Image Comput Comput Assist Interv 10(Pt 1):18–26
Kasprian G, Langs G, Brugger PC, Bittner M, Weber M, Arantes M, Prayer D (2011) The prenatal origin of hemispheric asymmetry: an in utero neuroimaging study. Cereb Cortex 21(5):1076–1083
Kazan-Tannus JF, Dialani V, Kataoka ML, Chiang G, Feldman HA, Brown JS, Levine D (2007) MR volumetry of brain and CSF in fetuses referred for ventriculomegaly. Am J Roentgenol 189(1): 145–151
Kostović I, Judas M (2002) Correlation between the sequential ingrowth of afferents and transient patterns of cortical lamination in preterm infants. Anat Rec 267(1):1–6
Kudelski D, Mari J.-L, Viseur S (2010) 3D Feature Line Detection based on Vertex Labeling and 2D Skeletonization. In: Proceedings of the 2010 Shape Modeling International Conference (SMI '10), vol 1. IEEE Computer Society, Washington, pp 246–250
Lee JK, Lee J-M, Kim JS, Kim IY, Evans AC, Kim SI (2006) A novel quantitative cross-validation of different cortical surface reconstruction algorithms using MRI phantom. Neuroimage 31(2): 572–584
Lefebvre J, Leroy F, Khan S, Dubois J, Hüppi P, Baillet S, Mangin JF (2009) Identification of growth seeds in the neonate brain through surfacic Helmholtz decomposition. Inf Process Med Imaging 21:252–256
Limperopoulos C, Clouchoux C (2009) Advancing fetal MRI: target for the future. Semin Perinatol 34(4):289–298
Limperopoulos C, Tworetzky W, McElhinney DB, Newburger JW, Brown DW, Robertson RL Jr, Guizard N, McGrath E, Geva J, Annese D, Dunbar-Masterson C, Trainor B, Laussen PC, du Plessis AJ (2010) Brain volume and metabolism in fetuses with congenital heart disease: evaluation with quantitative magnetic resonance imaging and spectroscopy. Circulation. 121(1):26–33
Lohmann G, Von Cramon Y, Colchester A (2007) Deep sulcal landmark provide an organizing framework for human cortical folding. Cereb Cortex 18(6):1415–1420
Luders E, Thompson PM, Narr KL, Toga AW, Jancke L, Gaser C (2006) A curvature-based approach to estimate local gyrification on the cortical surface. Neuroimage 29(4):1224–1230
Lyttelton O, Boucher M, Robbins S, Evans A (2007) An unbiased iterative group registration template for cortical surface analysis. Neuroimage 34(4):1535–1544
McDonald D, Kabani N, Avis D, Evans AC et al (2000) Automated 3-D extraction of inner and outer surfaces of cerebral cortex from MRI. Neuroimage 12(3):340–356
O'Rahilly R, Muller F (1999) The embryonic human brain: an atlas of developmental stages. John Wiley & Sons Ltd, Chichester
Prayer D (2006) Investigation of normal organ development with fetal MRI. Eur Radiol 17(10):2458–2471
Rajagopalan V, Scott J, Habas PA, Kim K, Corbett-Detig J, Rousseau F, Barkovich AJ, Glenn OA, Studholme C (2011) Local tissue growth patterns underlying normal fetal human brain gyrification quantified in utero. J Neurosci 31(8):2878–2887
Rakic P (1988) Specification of cerebral cortical areas. Science 241:170–176
Regis J, Mangin J, Ochiai T, Frouin V, Rivière D, Cachia A, Tamura M, Samson Y (2005) Sulcal roots generic model: a hypothesis to overcome the variability of the human cortex folding patterns. Neurol Med Chir 45:1–17
Richman DP, Stewart RM, Hutchinson JW, Caviness VS (1975) Mechanical model of brain convolutional development. Science. 189:18–21
Rivière D, Mangin J-F, Papadopoulos-Orfanos D, Martinez J-M, Frouin V, Regis J (2002) Automatic recognition of cortical sulci of the human brain using a congregation of neural network. Med Image Anal 6(2):77–92
Rössl C, Kobbelt L, Seidel HP (2000) Extraction of feature lines on triangulated surfaces using morphological operators. In: Proceedings of the AAAI Symposium on Smart Graphics, vol 4, pp 71–75
Rousseau O, Glenn B, Iordanova et al (2006) Registration-based approach for reconstruction of high-resolution in utero fetal mr brain images. Acad Radiol 13(9):1072–1081
Shankle WR, Landing BH, Rafii MS, Schiano A, Chen JM, Hara J (1998) Evidence for a postnatal doubling of neuron number in the developing human cerebral cortex between 15 months and 6 years. J Theor Biol 191(2):115–140
Sled JG, Zijdenbos AP, Evans AC (1998) A non-parametric method for automatic correction of intensity non-uniformity in MRI data. IEEE Trans Med Imaging 17(1):87–97
Thompson PM, Schwartz C, Lin RT, Khan AA, Toga AW (1996) Three-dimensional statistical analysis of sulcal variability in the human brain. J Neurosci 16(13):4261–4274
Toro R, Burnod Y (2003) Geometric atlas: modeling the cortex as an organized surface. Neuroimage 20(3):1468–1484
Van Essen D (1997) A tension-based theory of morphogenesis and compact wiring in the central nervous system. Nature. 385(23):313–318
Xu G, Knutsen AK, Dikranian K, Kroenke CD, Bayly PV, Taber LA (2010) Axon pull on the brain, but tension does not drive cortical folding. J Biomech Eng 132(7):071013
Yoshizawa S, Belyaev A, Seidel H (2005) Fast and robust detection of crest lines on meshes. In: Proceedings of the 2005 ACM symposium on Solid and physical modeling, pp 227–232
Zhang Y, Brady M, Smith S (2001) Segmentation of brain MR images through a hidden Markov random field model and the expectation maximization algorithm. IEEE Trans Med Imaging 20(1):45–57
Zhang Z, Liu S, Lin X, Sun B, Yu T, Geng H (2010) Development of fetal cerebral cortex: assessment of the folding conditions with post-mortem Magnetic Resonance Imaging. Int J Dev Neurosci 28(6):537–543
Zilles K, Amstrong E, Schleicher A, Kretschmann H (1988) The human pattern of gyrification in the human brain. Anat Embryol 179(2):173–179